**Reprinted from**

# AGRICULTURAL AND FOREST METEOROLOGY

*An International Journal*

Agricultural and Forest Meteorology 69 (1994) 223–245

# Radiative transfer in shrub savanna sites in Niger: preliminary results from HAPEX-Sahel. 1. Modelling surface reflectance using a geometric-optical approach

Janet Franklin*[,a], Jeff Duncan[a], Alfredo R. Huete[b], W.J.D. van Leeuwen[b], Xiaowen Li[c], Agnès Bégué[d]

[a]*Department of Geography, San Diego State University, San Diego, CA 92182, USA*
[b]*Department of Soil and Water Science, University of Arizona, Tucson, AZ 85721, USA*
[c]*Remote Sensing Centre, Boston University, Boston, MA 02215, USA*
[d]*Department of Geography, University of Maryland, College Park, MD 20742, USA*

(Received 26 February 1993; revision accepted 6 September 1993)

ELSEVIER

# AGRICULTURAL AND FOREST METEOROLOGY




**Scope of the journal**

*Agricultural and Forest Meteorology* is an international journal for the publication of articles and reviews in the interdisciplinary fields of meteorology and plant, animal and soil sciences as applied to heat, mass and momentum transfer in agriculture, forestry or natural ecosystems. Articles must appeal to an international audience. Emphasis is on basic and applied scientific research to problems in agriculture, forestry and natural ecosystems. Theoretical models should always be tested against experimental data. Typical topics include radiation transfer in plant canopies, evapotranspiration, energy transfer, air turbulence in and above plant canopies, forest-fire/weather interactions, pollutant fluxes to vegetation in the field and enclosures, trace gas fluxes in man-made and natural ecosystems, climatology of plant distributions, glasshouse energy balances and climatology, animal biometeorology. Special issues devoted to single topics, conference proceedings and comprehensive reviews are also published.


**Publication schedule and subscription information**

*Agricultural and Forest Meteorology* (ISSN 0168-1923). For 1994 volumes 68–72 are scheduled for publication. Subscription prices are available upon request from the Publisher. Subscriptions are accepted on a prepaid basis only and are entered on a calendar year basis. Issues are sent by surface mail except to the following countries where air delivery via SAL mail is ensured: Argentina, Australia, Brazil, Canada, Hong Kong, India, Israel, Japan, Malaysia, Mexico, New Zealand, Pakistan, PR China, Singapore, South Africa, South Korea, Taiwan, Thailand, USA. For all other countries airmail rates are available upon request. Claims for missing issues must be made within six months of our publication (mailing) date. Please address all your requests regarding orders and subscription queries to: Elsevier Science B.V., Journal Department, P.O. Box 211, 1000 AE Amsterdam, the Netherlands. Tel.: 31-20-5803642, Fax: 31-20-5803598. For further information, or a free sample copy of this or any other Elsevier Science journal, readers in the USA and Canada can contact the following address: Elsevier Science Inc., Journal Information Center, 655 Avenue of the Americas, New York, NY 10010, USA, Tel.: (212) 633-3750, Fax: (212) 633-3764.

**Back volumes** 1–10, 12–13, 15–52 are available. Price per volume: Dfl. 283.00 (approx. US$170.50) plus Dfl. 18.00 (US$8.90) p.p.h. per volume.

US mailing notice – *Agricultural and Forest Meteorology* (ISSN 0168-1923) is published monthly except for February, June and October by Elsevier Science B.V., (Molenwerf 1, Postbus 211, 1000 AE Amsterdam). Annual subscription price in the USA US $1070 (valid in North, Central and South America only), including air speed delivery. Application to mail at second class postage rate is pending at Jamaica, NY 11431. USA POSTMASTERS: Send address changes to *Agricultural and Forest Meteorology* Publications Expediting, Inc., 200 Meacham Avenue, Elmont, NY 11003. Airfreight and mailing in the USA by Publications Expediting.

ELSEVIER

Agricultural and Forest Meteorology 69 (1994) 223–245

AGRICULTURAL AND FOREST METEOROLOGY

# Radiative transfer in shrub savanna sites in Niger: preliminary results from HAPEX-Sahel. 1. Modelling surface reflectance using a geometric-optical approach

Janet Franklin*[,a], Jeff Duncan[a], Alfredo R. Huete[b], W.J.D. van Leeuwen[b], Xiaowen Li[c], Agnès Bégué[d]

[a]*Department of Geography, San Diego State University, San Diego, CA 92182, USA*
[b]*Department of Soil and Water Science, University of Arizona, Tucson, AZ 85721, USA*
[c]*Remote Sensing Centre, Boston University, Boston, MA 02215, USA*
[d]*Department of Geography, University of Maryland, College Park, MD 20742, USA*

(Received 26 February 1993; revision accepted 6 September 1993)

**Abstract**

To use optical remote sensing to monitor land surface–climate interactions over large areas, algorithms must be developed to relate multispectral measurements to key variables controlling the exchange of matter (water, carbon dioxide) and energy between the land surface and the atmosphere. The proportion of the ground covered by vegetation and the interception of photosynthetically active radiation (PAR) by vegetation are examples of two variables related to evapotranspiration and primary production, respectively. An areal-proportion model of the multispectral reflectance of shrub savanna, composed of scattered shrubs with a grass, forb or soil understory, predicted the reflectance of two 0.5 $km^2$ sites as the area-weighted average of the shrub and understory or 'background' reflectances. Although the shaded crown and shaded background have darker reflectances, ignoring them in the area-weighted model is not serious when shrub cover is low and solar zenith angle is small. A submodel predicted the reflectance of the shrub crown as a function of the foliage reflectance and amount of plant material within the crown, and the background reflectance scattered or transmitted through canopy gaps (referred to as a soil–plant 'spectral interaction' term). One may be able to combine these two models to estimate both the fraction of vegetation cover and interception of PAR by green vegetation in a shrub savanna.

* Corresponding author.


*SSDI* 0168-1923(93)02115-M

## 1. Introduction

The HAPEX-Sahel (Hydrologic Atmospheric Pilot Experiment) that took place during 1991–1993 is part of a major international research effort to study land surface climatology, and the exchange of mass and energy between the land surface and the atmosphere (André et al., 1988; Shuttleworth, 1991; Sellers et al., 1992; Bolle et al., 1993). The experiment is aimed at improving the parameterization of land surface–atmosphere interactions at the General Circulation Model (GCM) grid-cell scale (Goutorbe et al., 1993). The HAPEX-Sahel study area, located in Niger, West Africa, comprises a 1° latitude by 1° longitude square (13–14°N, 2–3°E). Components of energy, carbon and water balances were measured in three supersites within this study area using ground-based instruments and measurements, concentrating on the intensive observation period (IOP) of August–October 1992 (Goutorbe et al., 1993). One objective of HAPEX-Sahel was to develop algorithms for estimating surface parameters that are important in the land surface–atmosphere exchanges of energy and moisture in the subtropics from remotely sensed data (Prince et al., 1993).

A complementary objective is to validate a physiologically based model of primary productivity driven by the normalized difference vegetation index (NDVI) derived from coarse-resolution AVHRR (advanced very high resolution radiometer) satellite data (Prince, 1991). The NDVI exploits the contrast between the near-infrared (NIR) reflectance and the red absorption of green (photosynthetically active) vegetation. Plant photosynthesis is intimately linked to the carbon, oxygen and water cycles. One of the major land cover types in the study area is shrub savanna consisting of a sparse overstory of shrubs (bushes) and small trees with an understory of grasses or, in areas subject to sheet erosion, bare soil with some herbaceous annuals. In 1991, we made field measurements of vegetation cover (including shrub size and density), aboveground production, surface reflectance and photosynthetically active radiation (PAR) interception by shrubs in a degraded bushland and a bush/grassland site in Niger. This is the first in a series of three papers in which we discuss (1) the geometric-optical modelling of canopy reflectance (this paper), (2) PAR interception of the woody layer (Bégué et al., 1993), and (3) bidirectional reflectance characteristics and vegetation indices for monitoring primary production (Van Leeuwen et al., 1993).

Shrub cover affects the radiative transfer, and hence the relationship between primary productivity, absorbed PAR, and green vegetation indices in a number of ways. In addition to absorbing and scattering visible and NIR radiation with photosynthetically active green leaves, shrubs also (a) absorb PAR with non-photosynthetic branches, (b) cast shadows (intercept PAR that would otherwise have reached the understory or soil), and (c) scatter NIR radiation onto the understory or ground surface. The magnitude of these effects on canopy reflectance was explored by testing a simple, areal-proportion model of canopy reflectance which predicts the global reflectance of a site from the reflectances of vegetation and soil, weighted by their cover, with and without shadowing effects, predicted from crown geometry. A submodel which explicitly treats the spectral interaction between the shrub canopy and background was then tested. This submodel was used to predict reflectances of the

individual components (shaded and unshaded plant crown, and shaded background) that are used in the site-scale areal-proportion model.

## 2. Background

### 2.1. Areal-proportion site reflectance model

The four-component Li–Strahler discrete object canopy reflectance model used in this study (Li and Strahler, 1985) can be summarized as follows. The spatially averaged reflectance, $R_G$, of a pixel (ground resolution element in a digital image) or a group of pixels corresponding to a vegetation stand whose canopy consists of discrete crowns casting shadows on a contrasting, spectrally uniform background (continuous grass cover, soil, snow, etc.), can be modelled as the weighted average of four component reflectances:

$$R_G = (P_S R_S) + (P_Z R_Z) + (P_T R_T) + (P_C R_C) \tag{1}$$

where $P$ is the cover proportion, $R$ is the reflectance of sunlit background ($S$), shaded background ($Z$), shaded shrub crown ($T$), and sunlit shrub crown ($C$). In this paper, it is assumed the crowns are shrubs and the background is soil or herbaceous vegetation. A subscript for wavelength has been omitted for simplicity. We refer to a composite land surface consisting of discrete plant crowns over bare soil or an understory as a plant canopy (a discontinuous canopy) in order to be consistent with the literature, and we call this the site reflectance model.

The projected area of the crown component is equal to the sum of the shrub crown areas, $\sum_1^n \pi r^2$ (where $r$ is the radii of $n$ shrubs in the site), if the crowns are treated as spheroids and overlap is ignored. Crown cover can be estimated as the product of average crown area ($\overline{\pi r^2}$) and the average shrub density ($N$) per unit area if the variance of crown size is small. It was assumed that the shape of the shrubs in this study could be approximated to a spheroid (see Franklin and Turner, 1992), and the average canopy dimensions and solar zenith angle were used to estimate a geometric parameter, $\Gamma$, which we will refer to as a shadow cover index. The product $m\Gamma$ is the proportion of the area covered by shrub crown and its associated shadow, where $m$ can be thought of as a crown cover index equal to $\sum_1^n r^2/A$ ($A$ is the area of the site). The formula for $\Gamma$ for a spheroid is given in Strahler et al. (1988) and reproduced here for clarity

$$\Gamma = \pi + \pi/\cos\theta' - A_0 \tag{2}$$

where

$$A_0 = (\mathrm{B} - \frac{1}{2}\sin 2\mathrm{B})(1 + 1/\cos\theta')$$

if $(b + h)\tan\theta > r(1 + 1/\cos\theta')$, otherwise $A_0 = 0$. In this expression

$$B = \cos^{-1}\left[(1 + h/b)\left(\frac{1 - \cos\theta'}{\sin\theta'}\right)\right]$$

and

$$\theta' = \tan^{-1}[(b/r)\tan\theta]$$

where $r$ and $b$ are the horizontal and vertical radii of the spheroid, $h$ is the height of the spheroid above the ground, and $\theta$ is the solar zenith angle. (The stem height, $h$, is set to zero for a shrub.)

The proportions of the shrub plus shadow, the total figure ($m\Gamma$), which are crown ($K_C$), shaded crown ($K_T$), and shaded background ($K_Z$) (where $K_C$, $K_T$ and $K_Z$ sum to 1) can also be estimated from the geometry of the spheroid and the solar zenith angle as it was in Li and Strahler (1985) for a cone-shaped canopy.

For a spheroid

$$K_C = \frac{\pi/2(1 + \cos\theta')}{\Gamma}, \tag{3}$$

$$K_T = \frac{\pi/2(1 - \cos\theta')}{\Gamma}, \tag{4}$$

$$K_Z = \frac{\Gamma - \pi}{\Gamma}. \tag{5}$$

The cover proportions ($P$), which also must sum to 1, can be found from the following

$$P_S = 1 - m\Gamma \tag{6}$$

$$P_C = K_C m\Gamma \tag{7}$$

$$P_T = K_T m\Gamma \tag{8}$$

$$P_Z = K_Z m\Gamma \tag{9}$$

If the component reflectances are known, then Eq. (1) can be solved to estimate the stand or site reflectance in each waveband. Note that while the version of the model presented above assumes no overlapping of shrub crowns, the model has been modified further by Li and Strahler (1985, 1992) to account for changes in component proportions as a function of increasing crown overlap with cover.

### 2.2. Component reflectance submodel

Huete (1987) presented a model of the reflectance of a vegetated surface that approximates the first-order spectral interaction between an incomplete vegetation canopy and the soil background. He used this model to decompose canopy reflectance spectra into "a soil-dependent component and a vegetation component free of soil

influence" (Huete, 1987, p. 61). The vegetation canopy reflectance, $r_c$, can be expressed as

$$r_c = \rho_v c_v + \rho_s \tau_c^2 \tag{10}$$

where $\rho_v$ is the reflectance of the vegetation (plant parts), $c_v$ is the amount of vegetation in the sensor field of view (cover), $\rho_s$ is the soil reflectance and $\tau_c^2$ is the downward and upward global transmittance through the canopy. Global transmittance includes radiation reaching the soil surface by leaf transmission, plant scattering and penetration of direct and diffuse irradiance through canopy gaps. Upward and downward transmission are assumed to be equal and second-order interactions are ignored. Huete (1987) found that the soil-dependent contribution to canopy reflectance ($\rho_s \tau_c^2$) was significant when canopy cover was incomplete; soil-dependent canopy reflectance was greater in the NIR, which is strongly scattered by green vegetation, than in the visible wavelengths where the vegetation absorbs strongly.

The simple physical model behind Huete's formulation is a vegetation layer of small scattering elements covering a soil surface in a more or less uniform fashion. By way of leaf and gap transmission, beam and diffuse radiation penetrate the canopy, are scattered by the underlying soil layer, and are then transmitted upward to exit from the vegetation layer. This formulation also applies to a discontinuous plant canopy, such as a collection of sparse shrubs over a soil background. In this case, the transmission factor, $\tau_c$, includes geometric-optical effects such as those employed in the Li–Strahler model formulation.

Huete's (1987) first-order interaction model can also be extended to the crown and shaded components of the Li–Strahler model (1985) by calculating the component reflectances in Eq. (1) as follows

$$R_S \equiv \rho_s \tag{11}$$

$$R_C = \rho_v c_v + \rho_s \tau_c^2 \tag{12}$$

$$R_T = f_d(\rho_v c_v + \rho_s \tau_c^2) + (1 - f_d)\rho_s \tau_c^2 + (1 - f_d)\rho_v c_v \tau_c \tag{13}$$

$$R_Z = K_{open} f_d \rho_s + (1 - f_d)\rho_s \tau_c \tag{14}$$

where $f_d$ is the fraction of diffuse irradiance and $K_{open}$ is the proportion of diffuse irradiance reaching the shrub-shaded soil, on average, as a function of shrub height and density. In this case, $c_v$ is the projected vegetation cover within the perimeter of the plant crown (including foliage and branches in the case of shrubs), and $\tau_c$ measures the transmittance within that perimeter as well. Equations (11)–(13) taken together are referred to as the component submodel.

Equation (11) indicates that the soil background reflectance from Huete's notation ($\rho_s$) is equivalent to the sunlit soil reflectance ($R_S$) in the Li–Strahler formulation. Equation (12) applies Huete's model from Eq. (10) to the reflectance from the plant crown (the discrete clump of vegetation in the Li–Strahler model). Equation (13) states that the reflectance of the shaded crown component from Eq. (1) is equal to the diffuse irradiance ($f_d$) reaching the shaded portion of the crown and reflected

from it ($\rho_v c_v$), plus the direct beam irradiance ($1 - f_d$) transmitted through the crown and reflected from the soil ($\rho_s \tau_c^2$), plus that which is transmitted through the crown and reflected from the vegetation ($\rho_v c_v \tau_c$) on the shaded side. Equation (14) describes the reflectance from the soil shaded by the plant crown as the sum of the diffuse irradiance reaching the ground that is reflected by the soil ($K_{open} f_d \rho_s$) and the direct beam irradiance transmitted through the adjacent crown and reflected from the soil ($(1 - f_d)\tau_c \rho_s$). Note that these approximations for $R_T$ and $R_Z$ assume that only direct irradiance is transmitted through the canopy, and that diffuse skylight from the rest of the sky hemisphere also illuminates the shaded shrub crown and soil.

$K_{open}$ is used in $R_Z$ to adjust $f_d$ for the effect of surrounding shrub crowns ($f_d$ is not received from the entire hemisphere). It is approximated by calculating the between-crown gap probability over the entire sky hemisphere given the size and shape of the shrubs.

$$K_{open} = \int_0^{\pi/2} e^{-m\Gamma(\theta)} \sin\theta d\theta. \tag{15}$$

This effect is ignored in $R_T$ because it is more difficult to approximate and smaller in magnitude (because shaded shrub crown is, on average, higher off the ground surface and more open to skylight). Within this submodel, component reflectances are calculated more deterministically, as a function of vegetation and soil reflectances, within-crown cover and transmission, and geometric arrangement. The significance of the soil-dependent interaction terms in $R_C$, $R_T$ and $R_Z$ to the area-averaged site reflectance model would depend on their relative cover ($P_C$, $P_T$ and $P_Z$) as well as the vegetation cover within the perimeter of the crown, $c_v$, and the magnitude of the wavelength-dependent canopy transmittance, $\tau_c$.

Finally, we have only considered vertical interaction. With a canopy layer composed of discrete crowns, scattering from the crowns onto the adjacent background would increase the reflectance of the background near the crown perimeter and could contribute to area-averaged reflectance. Presumably this adjacency effect (or 'halo') would decay rapidly with distance from the canopy, even in the strongly scattering wavelengths.

## 3. Study area

The study sites were located in Niger, West Africa, near Ouallam (14°19′N, 1°58′E), about 100 km north of Niamey. The region experiences a short summer rainy season from June to September, and the average annual rainfall has been about 300 mm for the last 10 years (Institute National de Recherches Agronomiques du Niger (INRAN), unpublished data). The year the field data were collected (1991) was exceptionally wet with 510 mm rainfall for the season (INRAN, unpublished data).

This area is within the zone of rainfed agriculture, and the principal crop is pearl millet (*Pennisetum glaucum*). The landscape is a mosaic of a number of land cover types (Van Leeuwen et al., 1993) including millet and other cultivated fields, laterite-capped plateaus with 'tiger bush' (banded woody vegetation), and bush-fallow areas,

e.g. bushland or bush/grassland in various stages of secondary succession (Casenave and Valentin, 1989; Courault et al., 1990; Goutorbe et al., 1993). The bushland and bush/grassland (sometimes termed shrub savanna; Cole, 1986) would be the dominant natural vegetation type on the non-laterite areas in the absence of cultivation, and regenerates in areas that are left fallow (uncultivated). Areas left fallow for a short period (perhaps 1–3 years) are dominated by annual forbs and, after about 3–15 years, perennial grasses and shrubs regenerate (Courault et al., 1990). The distribution of vegetation types is determined by local site conditions, including soil texture, topographic position, and other factors affecting soil moisture availability (Justice and Hiernaux, 1986), as well as by land use.

Two contrasting bush fallow sites were chosen for study in 1991. Both sites have shrub canopies consisting almost exclusively of *Guiera senegalensis* with occasional *Combretum micranthum*, *C. glutinosum*, and other woody species. The bush/grassland site has an understory of perennial bunch grass (mainly *Aristida mutabulis* and *A. kerstingii* with some *Eragrostis tremula* and various forbs) while the degraded bushland site has been subjected to sheet erosion and the area between shrubs consists of exposed bare soil with some patchy annual forbs. Both sites were used for grazing by goats (*Guiera* and other shrubs were browsed), and the degraded bushland site for fuelwood collection, although living shrubs were not lopped (personal observation, 1991).

It was anticipated that these sites would serve as instrumented subsites during the 1992 HAPEX IOP, but travel restrictions made it impossible to work near Ouallam in 1992. However, the vegetation cover in the two sites is typical of the larger HAPEX study area. For example, land dominated by shrubs and perennial grasses (including bush/grassland, degraded bushland and the sandy skirts, or 'jupes sableuses', surrounding the laterite plateaus) were estimated to cover about 45% of a 400 $km^2$ area centred on the two shrub sites based on statistical classification of satellite multispectral data (J. Duncan and J. Franklin, unpublished data, 1992; note that those estimates were not quantitatively assessed by field sampling).

## 4. Methods

### *4.1. Shrub shape, size distribution and density, and vegetation cover*

For each of the two field sites, 250–350 measurements of shrub crown dimensions, the height and two diameters (the longest diameter and one perpendicular to it) were made in ten circular subplots (15 or 20 m radius) laid out on a regular grid (Fig. 1). Measurements were made on various dates between 27 July and 18 August 1991, with the assumption that shrub crown volume did not change greatly over this short interval (although some browsing and leaf growth did occur). These data, and the counts of shrubs within the subplots, were used to calculate shrub shape (characterized by the ratio of height to width), size and density per unit area. Cover of all major surface components was also estimated for each site along two parallel 1000-m transects, 75 m apart (described in Van Leeuwen et al., 1993) using the step-point

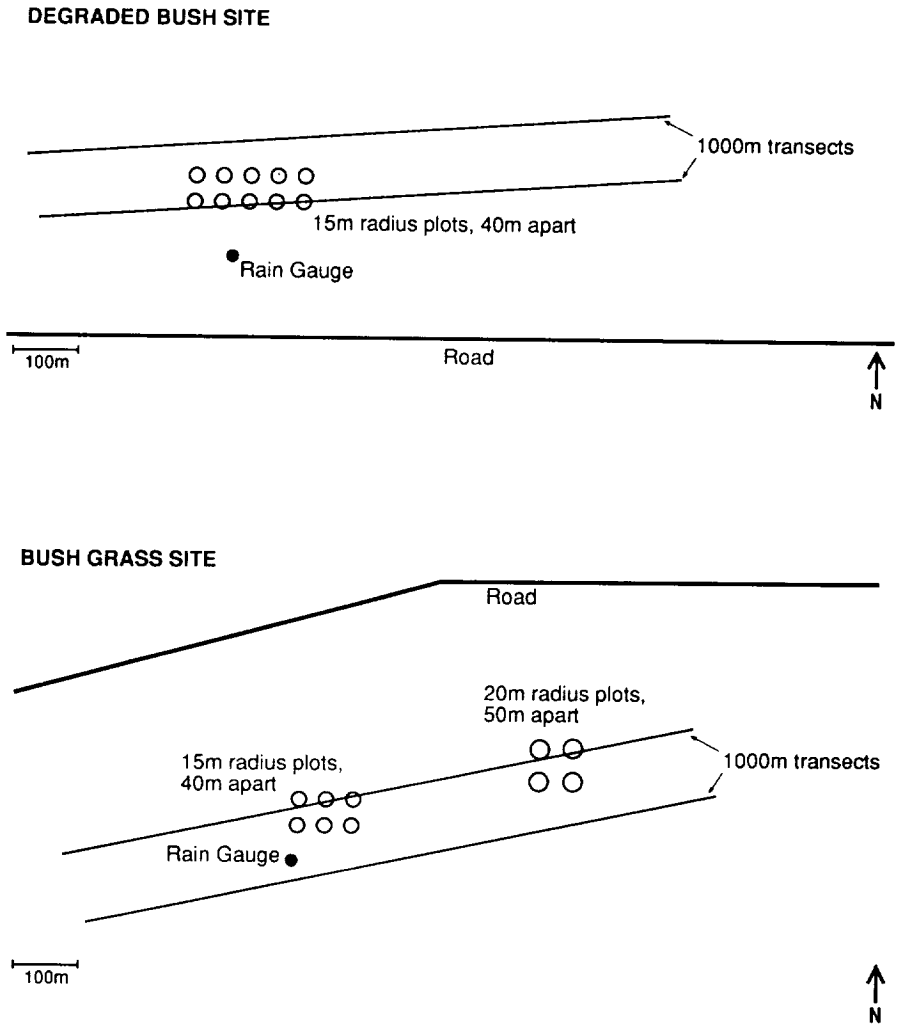


Fig. 1. Layout of subplots within (top) the degraded bushland site, and (bottom) the bush/grassland site. These subplots were used for measuring shrub size and density and component reflectances. Also indicated are the locations of the 1000-m transects used to characterize cover and reflectance for the sites.

method (Bonham, 1989). Multiple layers were recorded, but data presented in this paper only include the top layer, and therefore sum to 100% projected cover for the site. Cover categories included are: (1) bare soil; (2) grass; (3) forbs; (4) *Guiera* (the dominant shrub); (5) other shrubs (*Combretum micranthum*, *C. glutinosum*); (6) plant litter on the soil surface. Cover measurements were repeated during each of three sampling periods approximately 2 weeks apart during the growing season (Tables 1 and 2).

Table 1
Sample dates, local time and solar zenith angles ($\theta$) for shrub and site reflectance transects and cover measurements.

| | Sampling period | | | | | | | | |
|---|---|---|---|---|---|---|---|---|---|
| | 1 | | | 2 | | | 3 | | |
| | Date and time | No of shrubs | Solar zenith angle | Date and time | No of shrubs | Solar zenith angle | Date and time | No of shrubs | Solar zenith angle |
| *Bush/grassland* | | | | | | | | | |
| shrub reflectance | 1 Aug 91 | | | 10 Aug 91 | | | 22 Aug 91 | | |
| | 10:30 h | 20 | 36 | 15:30 h | 18 | 36 | 10:45 h | 23 | 32 |
| | 15:30 h | 24 | 36 | | | | | | |
| site reflectance | 30 Jul 91 | | | 15 Aug 91 | | | 25 Aug 91 | | |
| | 10:00 h | | 42 | 10:40 h | | 33 | 10:05 h | | 41 |
| site cover | 26 Jul 91 | | | 16 Aug 91 | | | 25 Aug 91 | | |
| *Degraded bushland* | | | | | | | | | |
| shrub reflectance | 28 Jul 91 | | | 9 Aug 91 | | | 23 Aug 91 | | |
| | 15:45 h | 19 | 40 | 11:00 h | 25 | 34 | 10:05 h | 24 | 41 |
| | | | | 16:10 h | 10 | 47 | | | |
| site reflectance | 29 Jul 91 | | | 15 Aug 91 | | | 25 Aug 91 | | |
| | 10:30 h | | 36 | 10:00 h | | 42 | 10:45 h | | 32 |
| site cover | 24 Jul 91 | | | 16 Aug 91 | | | 24 Aug 91 | | |

### 4.2. Component and site reflectances and vegetation indices

The reflectances of the four components were estimated based on field measurements using an Exotech radiometer (Exotech, Gaithersburg, MD, USA) and SPOT bandpass filters. Component radiances were sampled along short transects through individual shrubs oriented in the principal plane of the sun as described in Franklin and Turner (1992) and Franklin et al. (1993), and these will be referred to as the shrub reflectance transects (Fig. 2). The nominal height of the radiometer above the target

Table 2
Cover of the surface components (top layer only — non-overlapping cover) expressed as a proportion of the total transect length for each of the three sample periods

| Component | Bush/grassland | | | Degraded bushland | | |
|---|---|---|---|---|---|---|
| | 26 Jul 91 | 16 Aug 91 | 25 Aug 91 | 24 Jul 91 | 16 Aug 91 | 24 Aug 91 |
| Soil | 0.40 | 0.35 | 0.37 | 0.82 | 0.78 | 0.77 |
| Grass | 0.37 | 0.45 | 0.42 | 0.03 | 0.04 | 0.04 |
| Forb | 0.02 | 0.04 | 0.04 | 0.04 | 0.07 | 0.08 |
| *Guiera* | 0.07 | 0.07 | 0.05 | 0.10 | 0.09 | 0.10 |
| Other shrub | 0.02 | 0.00 | 0.00 | 0.00 | 0.00 | 0.00 |
| Litter | 0.13 | 0.11 | 0.11 | 0.01 | 0.04 | 0.04 |

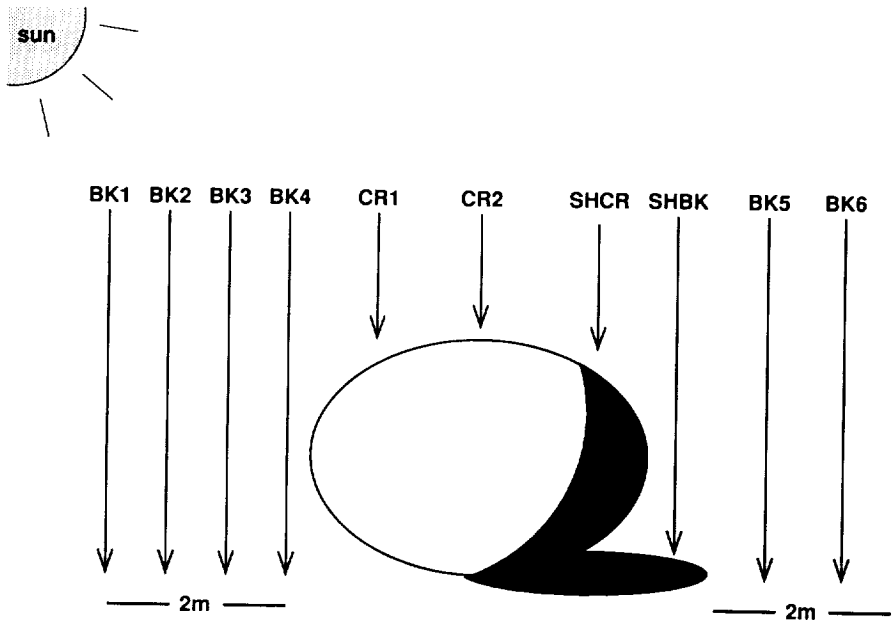


Fig. 2. Location of radiance measurements in shrub transects, where measurements are of background radiance (BK1-6); shrub crown (CR1-2); shaded shrub crown (SHCR); and shaded background (SHBK).

was 0.5–1.5 m and, with a 15° field-of-view lens, the footprint was 0.13–0.39 m in diameter. Observations made within each of the four components were averaged. This yielded 10–40 radiance observations per component in each site during each of three sampling periods (Table 1). The sampling scheme also allowed us to examine the data for evidence of scattering of radiation by the shrubs onto the adjacent ground. In addition, measurements of global or average site radiance were made along two 1000-m transects (the same ones used to make the cover estimates) using a yoke mount for the radiometer and taking measurements every 5 m from a height of 1.9 m, yielding a target diameter of 0.45 m (Van Leeuwen et al., 1993). All observations for the site were averaged. These transect-based site averages were used to validate the areal-proportion site reflectance model.

The 1000-m transect measurements were all made at approximately the same time of the morning (Table 1). The shrub transect measurements were taken between 10:00 and 11:00 h or 15:00 and 16:00 h local time, when the solar zenith angle ranged from 32° to 47° (Table 1). (While Van Leeuwen et al. (1993) noted that surface reflectance varied between morning and afternoon as the soil dried in a 20% grass cover site, we did not observe this pattern in the shrub transect data.) All radiance measurements were calibrated using measurements from a barium sulfate reference plate. Results are presented here for the red (0.61–0.68 $\mu$m) and NIR (0.79–0.89 $\mu$m) SPOT wavebands. In addition, the normalized difference vegetation index, NDVI = (NIR − red)/(NIR + red), and soil adjusted vegetation index, SAVI = [(NIR − red)/(NIR + red + $L$)](1 + $L$) where $L$ is a constant used to normalize for soil background effects

(Huete, 1988), were calculated for each of the components and for the site, based on red and NIR reflectance. (In this study, $L = 1$; see Franklin et al., 1993.)

### 4.3. Areal-proportion site reflectance model

The cover variable, $m$, was calculated from the sum of crown area in the subplots within each site. The shadow cover index, $\Gamma$, was calculated for each observation date based on the angle of the sun and the average height to diameter ratio of the shrubs measured in each site using Eq. (2). Then the proportions of the four components were estimated for each date from Eqs. (3)–(9). The estimates of shrub cover from the geometric model ($\pi m$) were compared with the independent estimates of shrub cover made by line intercept along the two 1000-m transects (Fig. 1) to make sure that estimates were reasonable (see Results). The modelled cover proportions were used with the sampled component reflectances from each date to estimate average red and NIR site reflectance for each date using Eq. (1). Background reflectance for the bush/grassland site was calculated from the weighted average of grass and soil reflectance, and the cover proportions from the 1000-m transects for each date (Table 2). This was considered to be a more reasonable estimate of the background reflectance for the whole site than background measured on the shrub reflectance transects because grass cover tended to be high adjacent to the shrubs.

The red and NIR site reflectances were also calculated based on the sunlit crown and background components only. The shrub cover proportion was assumed to be $m\pi$ and background cover $1 - m\pi$. The purpose of this was to determine the magnitude of the contribution of shaded component reflectances to site reflectance, and this will be referred to as the two-component model, while Eq. (1) describes the four-component model.

The vegetation indices (VIs), NDVI and SAVI were then calculated for each site from the predicted red and NIR reflectances based on the four component model from each date (see Hanan et al., 1991)

$$\mathrm{NDVI} = (R_{G,nir} - R_{G,red})/(R_{G,nir} + R_{G,red})$$

where $R_{G,red}$ is the red reflectance of the site, and $R_{G,nir}$ is the NIR reflectance of the site both calculated from Eq. (1).

### 4.4. Component reflectance submodel

The component submodel was used to predict the component reflectances, $R_C$, $R_T$ and $R_Z$ for the degraded bushland and bush/grassland sites using Eqs. (11)–(14). Red and NIR soil background reflectance, $R_{S,\lambda}$, were known from field measurements. Red and NIR reflectances from vegetation, $\rho_{v,\lambda}$, were sampled in 1992 at a similar site on 26 September. Approximately ten layers of foliage were cut and stacked, and the reflectance was measured immediately with the Exotech radiometer. Note that this 'pure' foliage/branch component reflectance does not account for the canopy architecture of an intact shrub, and that cutting can affect the NIR reflectance of leaves within minutes. We assumed that this did not occur in the sclerophyllous *Guiera*

leaves. The ratio of diffuse to direct irradiance, $f_{d,\lambda}$ was based on the literature (Rosenberg et al., 1983). Values of 0.2 and 0.1 were used for the red and NIR bands, reasonable values for a clear atmosphere (Dozier, 1981). (According to an empirical formula given in Bégué et al. (1993), $f_d$ for solar radiation in Niamey would be 0.22 for the average sun angle at which our measurements were taken.) $K_{open}$ was calculated based on the height and density of shrubs in the stands using Eq. (15).

The canopy transmittance, $\tau_c$, should vary as a function of foliage cover within the crown, $c_v$, and wavelength. Radiative transfer models have often treated this as exponential decay of radiation as a function of leaf area index (the density of scattering elements within the canopy layer) according to Beer's Law. In this study we relied on estimates of $c_v$ and $\tau_c$ based on Bégué's radiative transfer model for *Guiera*. These estimates were calculated from measurements of crown volume, leaf and stem area, and angle distribution functions (taken as uniform) on a sample of 56 shrubs (Bégué et al., 1993). We calculated $c_v$ for each shrub using their Eq. (4), a uniform element angle distribution, and setting leaf and stem transmissivity and solar zenith angle equal to zero. The red and NIR crown transmission ($\tau_{c,\lambda}$ termed 'porosity' in Bégué's model) was calculated for each shrub using leaf transmissivities 0.1 and 0.4, respectively. Their Eq. (5) was used to approximate the extinction coefficient for a uniform element angle distribution. Cover ($c_v$) was related to crown transmittance ($\tau_c$) by regression for each wavelength. The average size of the bushes at each site was then used to predict the average leaf and stem area indices (see Bégué et al., 1993), which were used, as described above, to calculate an average $c_v$ for each site. The regressions developed above were used to calculate $\tau_{c,\lambda}$ for the site. Estimates of component reflectances were compared to observations from the third sample date (nearest to the end of the growing season), because estimates of transmissivity were based on leaf and stem area sampled at the end of the growing season, and the measurements of vegetation reflectance ($\rho_v$) were also made towards the end of the growing season (in 1992).

## 5. Results

### 5.1. Shrub shape, size distribution, density, and vegetation cover

*Guiera* shrubs in the bush/grassland site were significantly larger than those in the degraded bushland site ($P < 0.0001$) and had higher leaf area index (Bégué et al., 1993), but their density was much lower and cover was slightly lower (Table 3). Shrub height and average diameter were normally to slightly lognormally distributed. Projected crown area, calculated from average radius, was lognormally distributed for both sites (Bégué et al., 1993). Shrub crown cover within each site was estimated from the geometric model by summing the projected crown areas for all shrubs measured in the subplots (note that this assumes no canopy overlap); it was 8% in the bush/grassland site and 9% in the degraded bushland site (Table 3).

Shrub cover sampled on the 1000-m transects for the whole site, about 6% for the bush/grassland site and 9.5% for the degraded bushland site (Table 2), was similar to

Table 3
Shrub size, shape and density for the bush/grassland and degraded bushland sites

| | Bush/grass ($n = 250$) | Degraded bush ($n = 351$) |
|---|---|---|
| Height (m) | 1.64 (0.44)[a] | 1.14 (0.35) |
| Diameter 1 (m)[b] | 2.14 (0.86) | 1.73 (0.71) |
| Diameter 2 (m) | 1.72 (0.75) | 1.43 (0.64) |
| H/D[c] | 0.93 (0.31) | 0.77 (0.25) |
| Density | 270 ha$^{-1}$ | 495 ha$^{-1}$ |
| Cover | 8.07% | 9.38% |

[a] Standard deviation in parentheses.
[b] Diameters 1 and 2 are the longest axis and the one perpendicular to it.
[c] H/D is the average height to diameter ratio.

the values estimated from the geometric model (Table 3), indicating that the subplots were representative of the sites and the geometric model was valid. The lower cover detected by the transect method in the bush/grassland site was probably due to the difference in the methods. The transect method counted gaps in the canopy which were encountered as background, while the geometric model estimated the projected crown area. There was an increase in the cover of forbs during the growing season in the bush/grassland and degraded bushland sites (Table 2). Grass cover increased in the bush/grassland site over the three sampling dates. *Guiera* cover decreased by a few per cent, probably due to browsing by goats (Table 2). Above-ground biomass was observed to increase for the grasses in the grass site, from 800 to 1700 kg ha$^{-1}$ dry matter (based on ten 0.16-m$^2$ samples per date; Van Leeuwen et al., 1993).

### 5.2. Component reflectances

The measured component reflectances show that in the bush/grassland site, where the background is about 50% grass cover (Table 2), the background contrasts somewhat to the shrub canopy and its associated shadowed components in the red band (Fig. 3). While the differences are small, they are significant (Bonferroni $P < 0.01$; all $P$ values reported are based on the Bonferroni adjustment; see Franklin et al. (1993) for discussion of multiple comparisons of means procedures in this context). In the degraded bushland site where the background in mainly soil the contrast is very strong (Fig. 4) and significant ($P < 0.01$). However, in both sites the background has NIR reflectance similar to or slightly higher than shrub crown (and the difference was not significant), even when the background is bare soil, and both are brighter than the shadowed components (Figs. 3 and 4). This is not an unusual pattern for bright soils in arid lands (Graetz and Gentle, 1982; Bégué and Prince, 1992; Franklin et al., 1993).

The NDVI and SAVI normalize for the effect of illumination and shadowing in that the VI values for the shaded components are similar to those of their sunlit counterparts (Fig. 4) although the pattern is less clear for the bush/grassland site

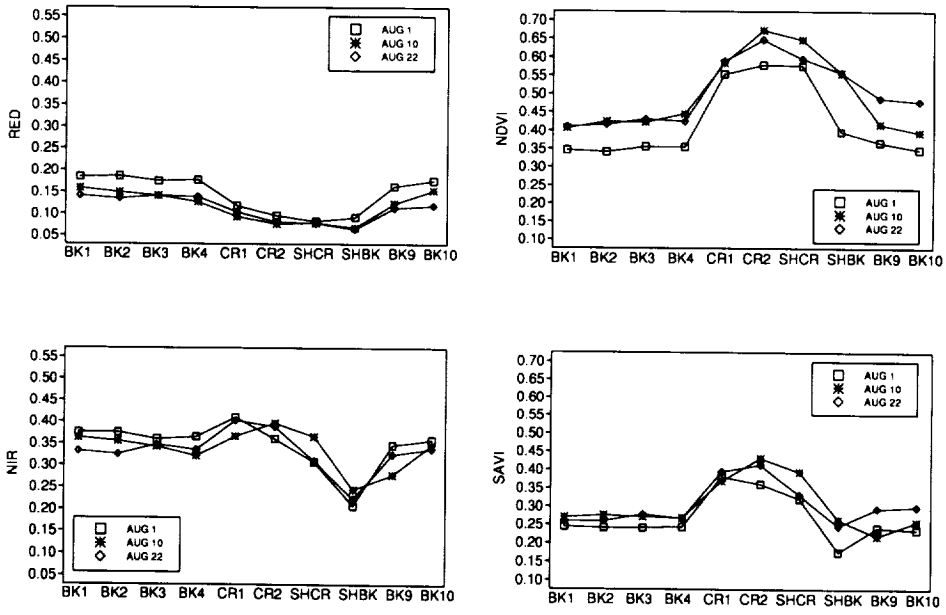


Fig. 3. Mean reflectances and VIs of each position on the shrub transects (Fig. 2) shown for three dates for the bush/grassland site. Refer to Fig. 2 for definitions of the reflectance components.

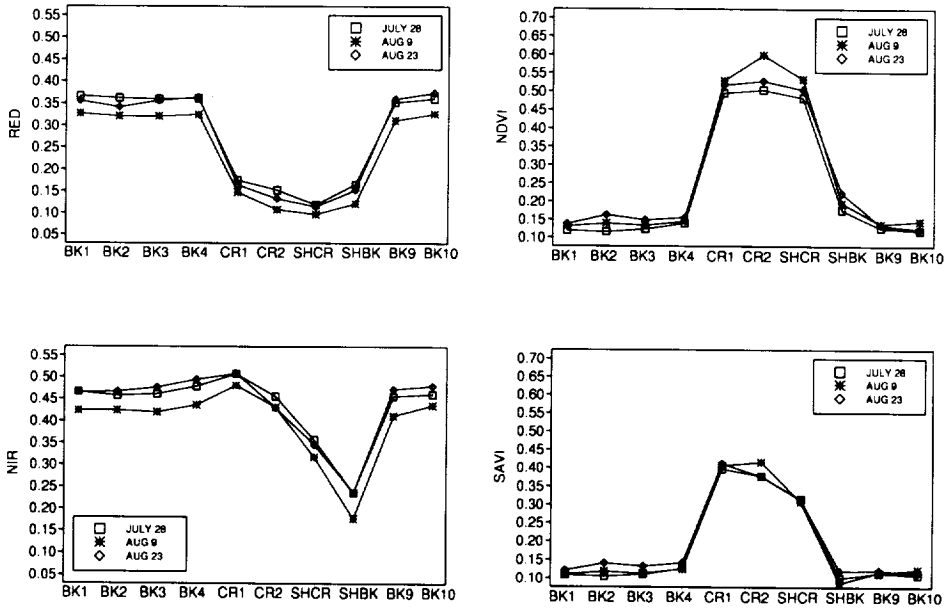


Fig. 4. Mean reflectances and VIs of each position on the shrub transects (Fig. 2) shown for three dates for the degraded bushland site. Refer to Fig. 2 for definitions of the reflectance components.

(Fig. 3) where the background is a variable mixture of soil and grass. While the NDVI of sunlit versus shadowed crown was not significantly different, the SAVI was in most cases; conversely, the NDVI of sunlit versus shadowed background was significantly different while the SAVI was not. The continuous nature of the variation in reflectance properties of the components is also apparent (Figs. 3 and 4). In the degraded bushland site there is very little temporal change in the greenness of the shrub canopies over the three dates (Fig. 4), but there is some evidence of the NIR 'halo' which is the increase in NIR reflectance from background (BK) measurements BK3 to BK4, causing a concurrent increase in VI values. While the magnitude of this effect is very small (the difference is not significant) and its influence is not seen very far from the shrub, it is seen consistently on all three dates. However, it could be safely ignored in the areal-proportion site reflectance model when woody cover is low. Perhaps it would contribute significantly to site reflectance at higher shrub cover (40–80%) than was found in these sites. Note that this effect cannot be detected in the bush/grassland site (Fig. 3).

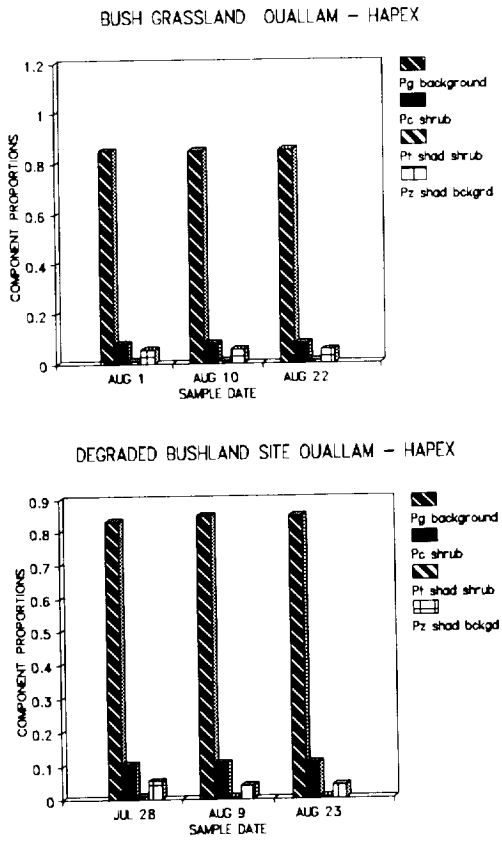


Fig. 5. Proportions of the four components ($P_G$, background; $P_C$, shrub crown; $P_T$, shaded shub crown; $P_Z$, shaded background) estimated from field measurements of shrub size, density, shape and solar zenith angle for each sample date.

### 5.3. Results of the areal-proportion site reflectance model

As noted above, estimates of shrub cover from the geometric model were very similar to transect estimates and so the modelled values are considered to be reasonable. The cover proportions for the four components estimated from the geometric model show that both sites are dominated by background (Fig. 5).

Figures 6 and 7 show the predicted and observed site reflectances and VIs for all dates. The results of the two- and four-component models are summarized using the mean of the absolute difference (MAD) of observed versus predicted reflectance, and the mean absolute proportion error (MAPE; the MAD divided by the observed reflectance) based on the six 'trials' (two sites on three dates) for each spectral band (Table 4). The overall MAPE for red and NIR is about 7–8%. Note that the site reflectances predicted from the two-component model is always higher than that

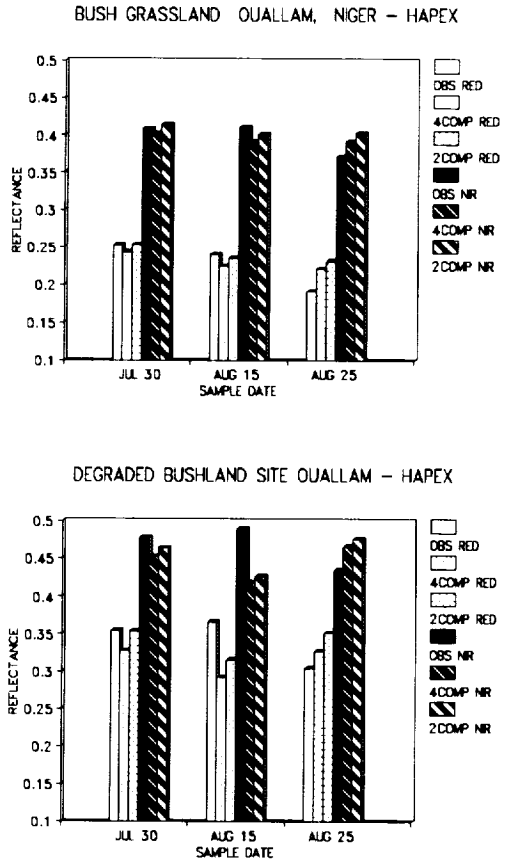


Fig. 6. Observed (OBS) and predicted red and NIR reflectance of the bush/grassland site (top) and the degraded bushland site (bottom) on three sample dates; observed site reflectance from the 1000-m transects, predicted site reflectance from the two-component (2COMP) and four-component (4COMP) areal proportion reflectance models.

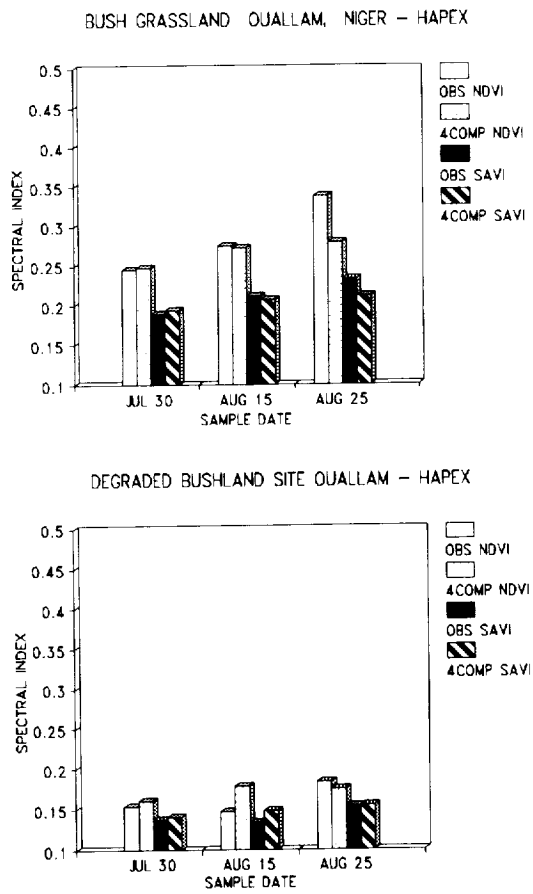


Fig. 7. Observed (OBS) and predicted NDVI and SAVI of the bush/grassland site (top) and the degraded bushland site (bottom) on three sample dates; observed site vegetation indices from the 1000-m transects, predicted site vegetation indices from the four-component (4COMP) areal proportion reflectance model.

Table 4
The mean absolute difference (MAD) and mean absolute per cent error (MAPE) of observed versus predicted site red and NIR reflectance for the four-component and two-component site reflectance model

| | Four-component | | Two-component | |
|---|---|---|---|---|
| | MAD | MAPE | MAD | MAPE |
| Red | 0.030 | 0.10 | 0.024 | 0.09 |
| NIR | 0.029 | 0.06 | 0.027 | 0.06 |
| Total | | 0.08 | | 0.07 |

predicted from the four-component model because the dark shadow components are ignored. The results of the two- and four-component models are essentially the same. This is because, while the shaded components are clearly 'darker' (Figs. 3 and 4), their areal proportions are very small (Fig. 5) owing to low shrub cover and moderate solar zenith angles.

There are several possible explanations for the difference between modelled and predicted site reflectances on some dates. It could be that the 1000-m transects used to characterize site reflectance and validate the model did not accurately estimate site reflectance due to sample variance. The lower red and NIR, and higher VIs, observed in the bush/grassland site on 25 August might have been incorrect. This is not likely as it is expected that VIs would increase, as observed, in this site due to the increasing grass biomass, and also that the moist soil background observed on the third date would cause lower reflectances and higher VIs (Van Leeuwen et al., 1993). The higher red and NIR, and slightly lower NDVI observed in the degraded bushland site on the second sampling date might have been incorrect due to differences in illumination conditions (although the zenith angle was actually larger; Table 1). However, the increase in green cover in the degraded site was very slight between the second and third dates, and the higher NDVI on the third date may have been a result of moister soil (Van Leeuwen et al., 1993).

It is also possible that the discrepancy between measured and modelled site reflectance was due to inaccurate characterization of component reflectances or cover used in the areal-proportion model. Cover estimates did not change very much between sampling dates, so it is more likely that estimation of component signatures, especially the background signature, is the problem. The difference between the observed and predicted site reflectance, seen in Figs. 6 and 7, is due almost entirely to the estimates of the background component reflectance because the background dominates the site cover (Fig. 5).

The two VIs, NDVI and SAVI, showed similar patterns. The observed values increased slightly during the observation period (Fig. 7) as the grass greened at the bush/grassland site and the forbs germinated at the degraded bushland site. While the SAVI is always lower in magnitude and range than the NDVI, the sensitivity of the VI cannot be based on its magnitude alone, but also on the magnitude of the 'noise' caused by soil background variation and viewing, and illumination geometry (Huete et al., 1993). It is not possible to tell from this study if the SAVI is exhibiting less sensitivity to soil background reflectance (but see Van Leeuwen et al. (1993)).

### *5.4. Results of the component reflectance submodel*

Input parameters for the component submodel are summarized in Table 5. The red and NIR crown transmissions were estimated from Bégué's model using the equations $\tau_{c,red} = (0.961 - 0.942c_v)^{0.564}$ ($r^2 = 0.91$), and $\tau_{c,nir} = (0.907 - 0.889c_v)^{0.384}$ ($r^2 = 0.91$). Estimated crown transmission values were similar to those measured for Sahelian tree species (Franklin et al., 1991) and lower in the red than the NIR band owing to greater NIR transmission by leaves. (In Franklin et al. (1991), red and NIR transmittances ranged from 0.55 to 0.85, but were roughly equal in the red and

Table 5
Parameters for and results of the component reflectance submodel

| | Degraded bushland | | Bush/grassland | |
|---|---|---|---|---|
| | Red | NIR | Red | NIR |
| *Input* | | | | |
| $\rho_v$ | 0.07 | 0.40 | 0.07 | 0.40 |
| $c_v$ | 0.76 | 0.76 | 0.87 | 0.87 |
| $\rho_s$ | 0.34 | 0.45 | 0.13 | 0.33 |
| $\tau_c$ | 0.46 | 0.57 | 0.34 | 0.47 |
| $f_d$ | 0.20 | 0.10 | 0.20 | 0.10 |
| $K_{open}$ | 0.77 | 0.77 | 0.77 | 0.77 |
| *Predicted* | | | | |
| $R_{C\,pred}$ | 0.12 | 0.45 | 0.07 | 0.42 |
| $R_{T\,pred}$ | 0.10 | 0.33 | 0.04 | 0.25 |
| $R_{Z\,pred}$ | 0.18 | 0.27 | 0.06 | 0.17 |
| *Observed*[a] | | | | |
| $R_{C\,obs}$ | 0.15 | 0.47 | 0.09 | 0.40 |
| s.d.[b] | (0.05) | (0.08) | (0.02) | (0.06) |
| $R_{T\,obs}$ | 0.12 | 0.35 | 0.08 | 0.31 |
| s.d. | (0.04) | (0.07) | (0.02) | (0.06) |
| $R_{Z\,obs}$ | 0.15 | 0.24 | 0.06 | 0.22 |
| s.d. | (0.05) | (0.05) | (0.02) | (0.04) |

[a] Observed values are from field data collected on 25 August 1991.
[b] s.d., standard deviations of field samples.

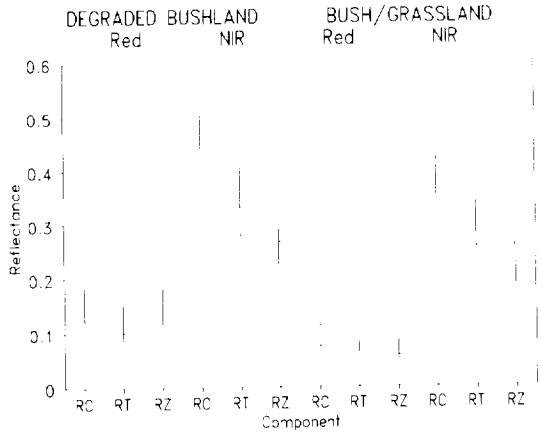


Fig. 8. Results of the component reflectance submodel for the three components, shrub crown ($R_C$), shaded shrub crown ($R_T$) and shaded background ($R_Z$). Vertical line shows the sample means of observed values for the last sample dates ± one standard deviation and horizontal dash shows the value predicted from the model for degraded bushland (left) and bush/grassland (right) red and NIR reflectance.

NIR, implying a larger contribution from canopy gaps.) The predicted reflectances for the crown and shaded components, $R_C$, $R_T$ and $R_Z$, usually fell within one standard deviation of the observed mean values measured on the third sample date for the two sites, 22 or 23 August, with the exceptions of $R_{T,red}$ and $R_{Z,nir}$ in the bush/grassland site (Fig. 8).

Figure 9 shows the modelled component signatures, $R_C$, $R_T$ and $R_Z$, when the foliage cover within the crown, $c_v$, varies from 10% to more than 90%, and the parameters from the degraded bushland site are used. This figure shows the non-linear change in component reflectances as a function of foliage cover, and hence wavelength-dependent canopy transmission. Sunlit crown reflectance ($R_C$) decreases rapidly in the red band as the foliage cover increases from 10 to 70% because canopy gaps are being filled. In the NIR band the sunlit crown reflectance is actually predicted to increase slightly with foliage cover (even though soil reflectance is greater than leaf reflectance) owing to canopy transmittance, which is still high (26%) when foliage cover is 98%. Shaded crown and background reflectance ($R_T$ and $R_Z$) decrease most rapidly in the NIR as cover increases from 70–100%, and the leaf transmission of the soil signal decreases in this single-scattering model. In the red band, shaded soil is always brighter than sunlit crown (because of the bright soil background), and shaded crown is always darker, while both decrease approximately linearly with foliage cover in this example. Unfortunately, without additional concurrent field measurements of leaf area and canopy reflectance, we were unable to validate this simulation over a wider range of cover values than are illustrated in Table 5 and Fig. 8.

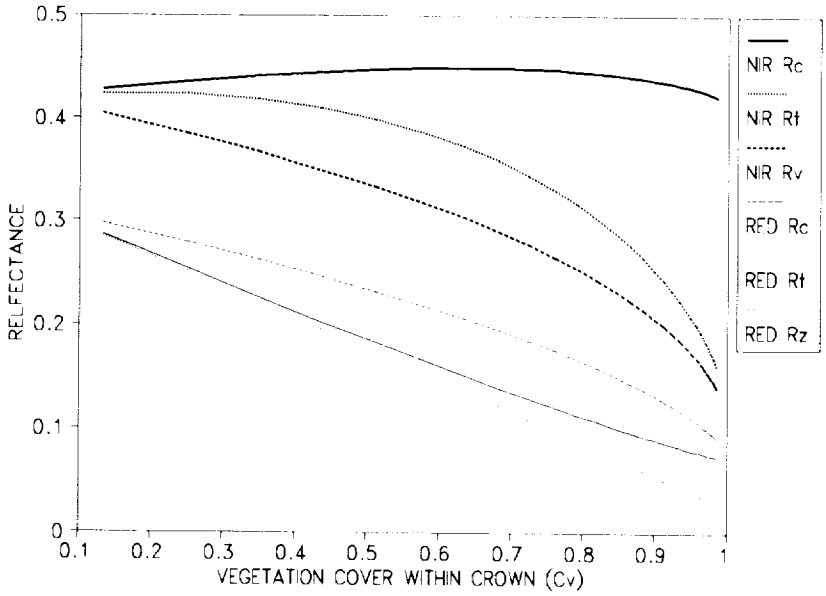


Fig. 9. Modelled values of red and NIR reflectance of the three components, shrub crown ($R_C$), shaded shrub crown ($R_T$) and shaded background ($R_Z$), for varying values of vegetation cover within the crown based on the parameters ($\rho_v$, $R_S$, $f_d$, $K_{open}$) from the degraded bushland site.

## 6. Discussion and conclusions

Sparse shrub savanna is an important land cover type in the West African Sahel, covering about half the land surface in some areas. The relative cover of shrubs, herbaceous plants and soil determine the partitioning of water (soil moisture, evapotranspiration) and energy (radiation balance), and thus affect land surface-atmosphere exchanges in the region. Remotely sensed estimates of vegetation cover and structure could be used in regional scale models of the effects of climate change on water and energy balance, and the carbon cycle.

In this study an areal-proportion model of the canopy reflectance of a shrub savanna predicted the surface reflectance as the weighted average of the component reflectances. A two-component model, including only shrub crown and background but ignoring shaded components, produced similar results to a four-component model that relies on three-dimensional crown geometry to estimate the area of shaded components. This is because, although the measured reflectances of shaded components were darker, in these sites shrub crown cover and density were low, so the shaded components have very small areas and contribute little to surface reflectance. This suggests that for the range of dates and zenith angles observed in this study, it may be possible to ignore a shade component when applying an areal-proportion model to satellite imagery of *Guiera* shrub savanna with shrub cover of less than 10%.

Two VIs, NDVI and SAVI, were also calculated from the modelled red and NIR reflectance for the sites and were similar to observed values. NDVI and SAVI showed the same pattern although SAVI was lower in magnitude and range. The VIs (observed and predicted) increased in value over the three sampling dates as the growing season progressed and green cover increased (Table 2). The third paper in this series discusses the sensitivity of the VIs to changes in soil brightness (Van Leeuwen et al., 1993).

The results of the areal-proportion model illustrate the need for more extensive and systematic sampling of component reflectances (especially the background) over a wider range of plant cover and illumination conditions in order to validate the model using satellite imagery. This has been carried out during the 1992 HAPEX field campaign, using hand-held, pole-mounted and airborne radiometers and a mast-mounted CCD (charge-coupled device) camera.

The component submodel was able to predict three component signatures as a function of vegetation cover within the crown and wavelength-dependent canopy transmission. This could be combined with the areal-proportion model to retrieve both canopy cover and vegetation cover within the crown. Presumably the latter is best related to vegetation amount (leaf area index or biomass), and thus to intercepted and absorbed PAR (Bégué et al., 1993). The component submodel could be extrapolated further to a discrete vegetation canopy layer (shrubs) over a continuous grass layer (continuous in its spatial distribution, but with less than 100% cover) over soil. Shrub canopy reflectance, for example, would then be

$$R_C = \rho_v c_v + \rho_h c_h \tau_c^2 + \rho_s \tau_c^2 \tau_h^2$$

where $\rho_h$, $c_h$ and $\tau_h^2$ are the reflectance, cover and two way transmittance of the

herbaceous layer (grass), respectively. This type of spectral interaction may be important in sites with higher shrub and grass cover, such as the central and southern supersites instrumented during the HAPEX-Sahel IOP.

In the HAPEX study area, for sites dominated by grass with low shrub cover (like the bush/grassland site), the first-order spectral interaction of the grass layer with underlying soil may contribute significantly to spectral response, and methods for correcting VI–APAR relationship for soil effect (including illumination-view angle effects) will be most useful (Huete, 1987, 1988; Huete et al., 1992; Van Leeuwen et al., 1993). In sites composed mainly of discrete plant canopies (like the degraded bushland site) or groups of canopies (tiger bush), or sites with both shrubs and grass but with higher shrub cover (10–40%), an areal-proportion model that includes geometric effects (shadows predicted from crown shape and illumination geometry), using the component submodel to predict the effects of crown structure on component reflectances, may be useful for retrieving vegetation parameters of interest. These parameters include shrub size and shape, and foliage density (leaf area or cover within the crown). Alternatively, if $c_v$ or $\tau_c$ could be estimated directly from multispectral (perhaps multiangle) imagery, by inversion of a model such as Bégué's, these quantities would be more directly related to APAR (and hence, primary productivity) than the cover of the Li–Strahler components.

## Acknowledgements

We are grateful to our colleagues Niall Hanan, Stephen Prince, and Alan Strahler for their contributions, including comments on the manuscript, and to Thierry Lebel and countless others who facilitated our HAPEX field work in Niger in 1991. This work was supported by NASA grants NAGW-2031 (to J. Franklin), NAGW-1949 (to A. Huete), NAGW-1967 and NAG 5-1471 (to S. Prince), and NSF grant INT-9014263 (to X. Li).

## References

André, J.-C. et al., 1988. HAPEX-MOBILHY: First results from the special observing period. Ann. Geophys., 6: 477–492.

Bégué, A. and Prince, S.D., 1992. Remote sensing of climate change in semi-arid lands using primary production of vegetation. In: Global Change and Education, ASPRS/ACSM/RT92, Washington, Dc, 1: 90–99.

Bégué, A., Hanan, N.P. and Prince, S.D., 1993. Radiative transfer in shrub savanna sites in Niger: preliminary results of HAPEX-Sahel. 2. Photosynthetically active radiation interception of the woody layer. Agric. For. Meteorol., 69: 247–266

Bolle, H.-J., André, J.-C., Arrue, J.L. et al., 1993. EFEDA: European field experiment in a desertification threatened area. Annal. Geophys., 11: 173–189.

Bonham, C.D., 1989. Measurements for Terrestrial Vegetation. Wiley, New York, 338 pp.

Casenave, A. and Valentin, C., 1989. Les états de surface de la zone Sahélienne: influence sur l'infiltration. Editions de l'ORSTOM, Paris, 229 pp.

Cole, M.M., 1986. The Savannas, Biogeography and Geobotany. Academic Press, London, 438 pp.
Courault, D., d'Herbes, J.-M. and Valentin, C., 1990. Le bassin versant de Sama Dey: premières observations pédologiques et phytoécologiques. Centre ORSTOM, Bondy, 36 pp.
Dozier, J., 1981. Energy and mass transfer in physical geography and remote sensing. Unpublished syllabus, Department of Geography, University of California, Santa Barbara, CA, 72 pp.
Franklin, J. and Turner, D., 1992. The application of a geometric optical canopy reflectance model to semiarid shrub vegetation. IEEE Geosci. Remote Sens., 30: 293–301.
Franklin, J., Prince, S.D., Strahler, A.H., Hanan, N.P. and Simonett, D.S., 1991. Reflectance and transmission properties of West African savanna trees from ground radiometer measurements. Int. J. Remote Sens., 12: 1369–1385.
Franklin, J., Duncan, J. and Turner, D., 1993. Reflectance of vegetation and soil in Chihuahuan desert plant communities from ground radiometry using SPOT wavebands. Remote Sens. Environ., in press.
Goutorbe, J.-P., et al., 1993. HAPEX-Sahel: A large-scale study of land–atmosphere interactions in the semi-arid tropics. Ann. Geophys., in press.
Graetz, R.D. and Gentle, M.R., 1982. The relationship between reflectance in the Landsat wavebands and the composition of an Australian semi-arid shrub rangeland. Photogramm. Eng. Remote Sens., 48:1721–1730.
Hanan, N.P., Prince, S.D. and Hiernaux, P.H.Y., 1991. Spectral modelling of multicomponent landscapes in the Sahel. Int. J. Remote Sens., 12: 1243–1258.
Huete, A.R., 1987. Soil-dependent spectral response in a developing plant canopy. Agron. J., 79: 61–68.
Huete, A.R., 1988. A soil-adjusted vegetation index (SAVI). Remote Sens. Environ., 25: 295–309.
Huete, A.R., Hua, G., Qi, J., Chebouni, A. and van Leeuwen, W.J.D., 1992. Normalization of multidirectional red and NIR reflectances with the SAVI. Remote Sens. Environ., 40: 1–20.
Huete, A.R., Justice, C. and Liu, H., 1993. Development of vegetation and soil indices for MODIS-EOS. Remote Sens. Environ., in press.
Justice, C.O. and Hiernaux, P.H.Y., 1986. Monitoring the grasslands of the Sahel using NOAA/AVHRR data. Int. J. Remote Sens., 7: 1475–1497.
Li, X. and Strahler, A.H., 1985. Geometric-optical modeling of a coniferous forest canopy. IEEE Tran. Geosci. Remote Sens., 23: 207–221.
Li, X. and Strahler, A.H., 1992. Geometric-optical bidirectional reflectance modeling of the discrete crown vegetation canopy: effect of crown shape and mutual shadowing. IEEE Tran. Geosci. Remote Sens., 30: 276–292.
Prince, S.D., 1991. A model of regional primary productivity for use with coarse resolution satellite data. Int. J. Remote Sens., 29: 1313–1330.
Prince, S.D. et al., 1993. Geographical, biological and remote sensing aspects of the Hydrologic Atmospheric Pilot Experiment in the Sahel (HAPEX-Sahel). Remote Sens. Environ., in press.
Rosenberg, N.J., Blad, B.L. and Verma, S.B., 1983. Microclimate: The Biological Environment. 2nd Edn., Wiley, New York, 495 pp.
Sellers, P.J., Hall, F.G., Asrar, G., Strebel, D.E. and Murphy, R.E., 1992. An overview of the First International Satellite Land Surface Climatology Project (ISLSCP) Field Experiment (FIFE). J. Geophys. Res., 97: 18345–18373.
Shuttleworth, W.J., 1991. Insights from large-scale observational studies of land–atmosphere interactions. Surv. Geophys., 12: 3–30.
Strahler, A.H., Wu, Y. and Franklin, J., 1988. Remote estimation of tree size and density from satellite imagery by inversion of a geometric-optical canopy model. Proc. 22nd Int. Symp. Remote Sensing Environment (20–26 October 1988, Abidjan, Ivory Coast). ERIM, Ann Arbor, MI, pp. 337–348.
Van Leeuwen, W.J.D., Huete, A.R., Duncan, J. and Franklin, J., 1993. Radiative transfer in shrub savanna sites in Niger: preliminary results of HAPEX-Sahel. 3. Optical dynamics and vegetation index sensitivity to biomass and plant cover. Agric. For. Meteorol., 69: 267–288.

## GENERAL INFORMATION

A detailed *Guide for Authors* is available upon request, and will also be printed in the first issue to appear in each year's subscription. You are kindly asked to consult this guide. Please pay special attention to the following notes.

*Language*

The official language of the journal is English, but occasional articles in French and German will be considered for publication. Such articles should start with an abstract in English, headed by an English translation of the title. An abstract in the language of the paper should follow the English abstract. English translations of the figure captions should also be given.

*Preparation of the text*

a) The manuscript should be typewritten with double spacing and wide margins and include at the beginning of the paper an abstract of not more than 500 words. Words to be printed in italics should be underlined. The metric system should be used throughout.

b) The title page should include: the title, the name(s) of the author(s) and their affiliations.

*References*

a) References in the text start with the name(s) of the author(s), followed by the publication date in parentheses.

b) The reference list should be in alphabetical order and on sheets separate from the text.

*Tables*

Tables should be compiled on separate sheets. A title should be provided for each table and they should be referred to in the text.

*Illustrations*

a) All illustrations should be numbered consecutively and referred to in the text.

b) Drawings should be completely lettered, the size of the lettering being appropriate to that of the drawings, but taking into account the possible need for reduction in size (preferably not more than 50%). The page format of *Agricultural and Forest Meteorology* should be considered in designing the drawings.

c) Photographs must be of good quality, printed on glossy paper.

d) Figure captions should be supplied on a separate sheet.

*Proofs*

One set of proofs will be sent to the author, to be checked for printer's errors. In the case of two or more authors please indicate to whom the proofs should be sent.

*Submission of manuscripts*

For North America: Dr. Kyaw T. Paw U, LAWR, Atmospheric Sciences, Hoagland Hall, University of California, Davis, CA 95616, USA

For Europe, Africa and the Middle East: Dr. James R. Milford, Department of Meteorology, University of Reading, 2, Earley Gate, Reading RG6 2AU, UK

For Asia, Australia, New Zealand, Central and South America: Dr. Ray Leuning, Centre for Environmental Mechanics, G.P.O. Box 821, Canberra, A.C.T. 2601, Australia

A manuscript rejected for publication in *Agricultural and Forest Meteorology* may not be resubmitted.

Manuscript and illustrations should be submitted in triplicate. One set should be in a form ready for reproduction: the other two may be of lower quality. Submission of an article is understood to imply that the article is original and unpublished and is not being considered for publication elsewhere. Upon acceptance of an article by the journal, the author(s) will be asked to transfer the copyright of the article to the publishers. This transfer will ensure the widest possible dissemination of information.

*Submission of electronic text*

In order to publish the paper as quickly as possible after acceptance, authors are encouraged to submit the final text also on a 3.5" or 5.25" diskette. Both double density (DD) and high density (HD) diskettes are acceptable. Make sure, however, that the diskettes are formatted according to their capacity (HD or DD) before copying the files onto them. Similar to the requirements for manuscript submission, main text, list of references, tables and figure legends should be stored in separate text files with clearly identifiable file names. The format of these files depends on the word processor used. Texts made with DisplayWrite, MultiMate, Microsoft Word, Samna Word, Sprint, Volkswriter, Wang PC, WordMARC, WordPerfect, Wordstar, or supplied in DCA/RFT, or DEC/DX format can be readily processed. In all other cases the preferred format is DOS text or ASCII. It is essential that the name and version of the wordprocessing program, type of computer on which the text was prepared, and format of the text files are clearly indicated. Authors are encouraged to ensure that **the disk version and the hardcopy must be identical**. Discrepancies can lead to proofs of the wrong version being made.



0168-1923/94/$07.00



This issue is printed on acid-free paper.

PRINTED IN THE NETHERLANDS